

Smart DIPSS for Dynamic Stability Enhancement on Multi-Machine Power System

Herlambang Setiadi¹, Fakhruddin Arrazi², Muhammad Abdillah³, Awan Uji Krismanto⁴

¹Faculty of Advanced Technology and Multidiscipline, Universitas Airlangga, Indonesia

²PT PG Rajawali II, Indonesia

³Department of Electrical Engineering, Universitas Pertamina, Indonesia

⁴Department of Electrical Engineering, Institut Teknologi Nasional, Indonesia

Article Info

Article history:

Received Oct 7, 2021

Revised Jan 17, 2022

Accepted Feb 21, 2022

Keyword:

ACO

Clean energy technology

DIPSS

Stability

Multimachine

ABSTRACT

Disruption of the electric power system always results in instability. These disturbances can be in the form of network breaks (transients) or load changes (dynamic). Changes in load that occur suddenly and periodically cannot be responded well by the generator so that it can affect the dynamic stability of the system. This causes the occurrence of frequency oscillations in the generator. A poor response can cause frequency oscillations for a long period. This will result in a reduction in the available power transfer power. In a multi-machine power system, all the machines work in synchrony, so the generator must operate at the same frequency. Therefore, disturbances that arise will have a direct impact on changes in electrical power. In addition, changes in electrical power will have an impact on mechanical power. The difference in response speed between a fast electrical power response and a slower mechanical power response will result in instability. As a result of these differences, the system oscillates. The addition of the excitation circuit gain is less able to stabilize the system. To solve the problem, additional signal changes are required. The additional signal is generated by the Dual Input Power System Stabilizer (DIPSS) setting using the Ant Colony Optimization (ACO) method. Three generator nine bus is used as the test system of this paper. Time domain simulation is used to investigate the efficacy of the proposed method. From the simulation results it is found that the proposed method is superior compared to the other scenarios. This indicated by the overshoot and the settling time of three generator are smaller compared to the other scenarios.

Copyright © 2022 Institute of Advanced Engineering and Science.
All rights reserved.

Corresponding Author:

Herlambang Setiadi,

Faculty of Advanced Technology and Multidiscipline,

Universitas Airlangga,

Campus C UNAIR Gedung Kuliah Bersama, Mulyorejo, Surabaya, Indonesia.

Email: h.setiadi@ftmm.unair.ac.id

1. INTRODUCTION

An electrical power system that is experiencing interference will result in system instability. The disturbance can be in the form of a sudden increase and decrease in load, network breaks, overload, or short circuit. Changes in the load that occur suddenly and periodically cannot be responded to properly by the generator so that it can affect the dynamic stability of the system [1]. This causes the occurrence of frequency oscillations in the generator. A poor response can cause frequency oscillations for a long period. This will result in a reduction in the available power transfer power. The problem will be more complicated if the system has more than one machine or multi-machine [2], [3].

A multi-engine system combines several generators (can consist of a coupled engine or a single engine) that are interconnected [4], [5]. In a multi-machine power system, all the machines work in synchrony, so the generator must operate at the same frequency. Instability is generally affected by the initial conditions and the magnitude of the disturbance. The disturbances that arise then have a direct impact on changes in electrical power [6]. Changes in electrical power will have an impact on mechanical power. The difference in response speed between a fast electrical power response and a slower mechanical power response will result in instability. As a result of these differences, the system experiences oscillations [7].

The dynamic stability of the electric power system is a stability study with the assumption that the governor response has little effect. This is because the governor response compared to the excitation system response is very slow. So that in dynamic stability, the controller that has an effect is the excitation system. The addition of the excitation circuit gain is less able to stabilize the system, especially during peak loads. Additional signal changes to increase attenuation at peak load conditions can solve this problem [8].

One of the methods used to increase this damping and stabilize the system is by adding additional controller such as power system stabilizer (PSS). Research effort in [9], shows that PSS can be used to enhance the dynamic stability of power system in present of renewable power generation. The application of PSS for enhancing stability of power system is reported in [10]. In [10], PSS is added in Kalimantan Selatan-Tengah and Kalimantan Timur interconnected system to stabilize the system. The application of PSS for low frequency oscillation is reported in [11]. It was found that PSS can damp the weak modes in interconnected power system. However, improper use of additional equipment in the electric power system will cause many problems. With these conditions, additional equipment is proposed in the form of a Dual Input Power System Stabilizer (DIPSS). In using DIPSS, optimal parameter tuning is very influential in stabilizing the system. However, the range of equipment parameters is very diverse and wide, so to quickly obtain parameter values, an optimization method using the Ant Colony Optimization (ACO) method is used.

2. SYSTEM MODEL AND ALGORITHM

2.1. Synchronous Machine Field Modeling

The synchronous machine model refers to the single machine model with infinite buses introduced by De Mello and Concordia, later developed by Mousa and Y.N. Yu became a multi-machine model that has become an IEEE standard [12]. The linear model of the synchronous machine includes the torque equation model and the field equation. The relationship between the change in the power angle and the change in flux velocity can be written in the form of a differential equation as described in (1) and (2) [13], [14] (see Appendix for each symbols):

$$\dot{\delta}_i = \omega_{0i} \Delta\omega_i \quad (1)$$

$$\Delta\dot{\omega}_i = \frac{1}{M_i} (T_{mi} - T_{ei} - D_i \Delta\omega_i) \quad (2)$$

The mathematical representation T_{ei} can be expressed by using (3). The parameters in Equation (3) can be described using (4), (5), (6), and (7) [13], [15].

$$\Delta T_{ei} = K_{1,ii} \Delta\delta_i + K_{2,ii} \Delta E'_{qi} - \sum_{j \neq i} K_{1,ij} \Delta\delta_j - \sum_{j \neq i} K_{2,ij} \Delta E'_{qj} \quad (3)$$

$$K_{1,ij} \neq \sum_{i \neq j} K_{1,ij} \quad (4)$$

$$K_{2,ii} = E'_{qi} G_{ii} - \sum_{i \neq j} E'_{qi} Y_{ij} \cos(\beta_{ii} + \delta_{ij}) K_{1,ij} \quad (5)$$

$$K_{1,ij} = E'_{qi} E'_{qj} Y_{ij} \sin(\beta_{ij} + \delta_{ij}) \quad (6)$$

$$K_{2,ij} = E'_{qi} E'_{qj} Y_{ij} \sin(\beta_{ij} + \delta_{ij}) \quad (7)$$

The i -th machine field equation in the form of a linear model can be written as (8) and (9) [16].

$$T'_{d0i} \Delta E_{qi} = \Delta V_{FDi} - \Delta E_{qi} - (x_{di} + x'_{di}) \Delta \Delta_{di} \quad (8)$$

$$\Delta \dot{E}_{qi} = -\Delta \frac{d}{dt} E'_{qi} \quad (9)$$

With

$$\Delta i_{di} = -\sum_{j \neq i} E'_{qi} y_{ij} \cos(\beta_{ij} + \delta_{ij}) \Delta \Delta_{ij} - B_{ii} E'_{qi} - \sum_{j \neq i} y_{ij} \sin(\beta_{ij} + \delta_{ij}) E'_{qj} \quad (10)$$

B_{ii} = i -th machine admittance imaginary component. Substituting the equation i_{di} into equation (10) produces equation (11) [16].

$$T'_{d0i} \Delta \dot{E}'_{qi} = \Delta V_{FDi} - C_{3,ii} \Delta E'_{qi} + K_{4,ii} \Delta \delta_i + \sum_{j \neq i} C_{3,ij} E'_{qj} - \sum_{j \neq i} K_{4,ij} \Delta \delta_j \quad (10)$$

With

$$C_{3,ii} = 1 - (x_{di} - x'_{di}) B_{ii} \quad (11)$$

$$K_{4,ii} = \sum_{j \neq i} K_{4,ij} \quad (12)$$

$$C_{3,ij} = (x_{di} - x'_{di}) y_{ij} \sin(\beta_{ij} + \delta_{ij}) \quad (13)$$

$$K_{4,ij} = (x_{di} - x'_{di}) E'_{qi} y_{ij} \cos(\beta_{ij} + \delta_{ij}) \quad (14)$$

2.2. Excitation System Model

The excitation system consists of a field circuit and a voltage regulator called the Automatic Voltage Regulator (AVR). The function of the excitation system is to supply flux to the generator and a field voltage regulator [13]. Equations (15)-(17) are showing the dynamic model of the excitation system.

$$\Delta \dot{V}_{FDi} = \frac{\Delta V_{Ai}}{T_{Ei}} - \frac{K_{Ei} \Delta V_{FDi}}{T_{Ei}} \quad (15)$$

$$\Delta \dot{V}_{Fi} = \frac{K_{Fi} \Delta V_{Ai}}{T_{Ei} T_{Fi}} - \frac{K_{Ei} K_{Fi} \Delta V_{FDi}}{T_{Ei} T_{Fi}} - \frac{K_{Fi}}{T_{Fi}} \quad (16)$$

$$T_{Ai} \Delta \dot{V}_{Ai} = \Delta U_{2i} K_{Ai} - \Delta V_{Fi} K_{Ai} - \Delta V_{Ai} - V_i K_{Ai} \quad (17)$$

2.3. Governor Model

The steam turbine has input in the form of mechanical energy emitted from the steam boiler and has an output of mechanical energy (torque) used to drive the steam turbine. The turbine model and control system here refer to the IEEE standard model [13]. Equations (18) and (19) are illustrated the dynamic model of governor used in this paper.

$$\Delta \dot{T}_{mi} = \left(\frac{2}{T_{wi}} + \frac{2}{T_{gwi}} \right) \Delta Y_i - \frac{2K_{gwi} \Delta U_{1i}}{T_{gwi}} + \frac{2K_{gwi} \Delta \omega_i}{R_i T_{gwi}} - \frac{2\Delta T_{mi}}{T_{wi}} \quad (18)$$

$$\Delta \dot{Y}_i = \frac{K_{gwi}}{T_{gwi}} \Delta U_{1i} + \frac{K_{gwi} \Delta \omega_i}{R_i T_{gwi}} - \frac{\Delta Y_i}{T_{gwi}} \quad (19)$$

2.4. Dual Input Power System Stabilizer

Power System Stabilizer (PSS) is a device that produces a control signal to be fed to the excitation system. The function of the PSS is to increase the stability limit by adjusting the generator excitation to provide damping for the rotor oscillations of the synchronous machine [17].

Dual Input Power System Stabilizer (DIPSS) is a type of PSS that can reduce signal noise [18]. However, this noise signal will result in an input reference error for the system. This noise signal can come from shaft motion such as lateral shaft run out, which causes overmodulation of the generator excitation system, or it can also come from torsional oscillations caused by changes in electrical torque.

This noise component will affect the excitation of the generator and affect the electrical torque. The input of this type of stabilizer is the change in rotor angular speed ($\Delta \omega$) and the change in electrical power (ΔPe). Each input signal is passed into the washout and transducer circuits. The washout circuit provides continuous conditions at the output of the stabilizer while the transducer is used to convert the input signal into a voltage signal. The DIPSS model is taken from the IEEE PSS2B type [19], [20]. The complete form of the DIPSS modeling is shown in Figure 1.

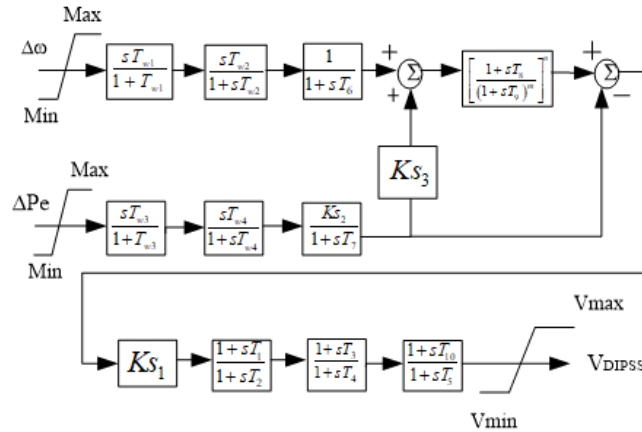


Figure 1. Block diagram of dual input power system stabilizer (IEEE type PSS2B)

2.5. Ant Colony Optimization (ACO)

Ant Colony Optimization (ACO) was first introduced by Marco Dorigo around 1990. ACO is an algorithm development inspired by the behavior of ant colonies in finding the shortest path between the nest and food [21]. Ants live in colonies, and their behavior is based on the behavior of living in colonies rather than working individually. Individual ants are useless. When working in colonies, ants can carry out a job effectively. For example, when looking for food sources from the nest, ants will be able to find where the food is and find the shortest path to get it and bring it to the nest. Ants can also adapt to changes when the old path is not possible or is hit by obstacles [22].

Ants provide information to each other using pheromones. Each time they pass a path, the ant will leave a pheromone, which stimulates the attraction of other ants to pass the same path. The next ant that passes through the path can identify the pheromone that is placed and decides to choose that path with a high probability and strengthens it with the pheromone it has. This basic trait can explain how ants find the shortest path and reconnect the broken path when hit by an obstacle. An indirect form of communication using pheromones is called stigmergy [23]. The more pheromones left behind the more ants that pass through a path. Pheromone levels in the path that many ants pass will increase, while the path that ants rarely pass will experience evaporation. This is because ants will choose a short path to get to the food. Therefore, more pheromones will be left behind, and the evaporation process will be short because the ants will return to the nest through the same path as leaving the pheromones back. In contrast, the long path will experience rapid evaporation because the pheromone levels are low due to the small number of ants that pass through the path [23].

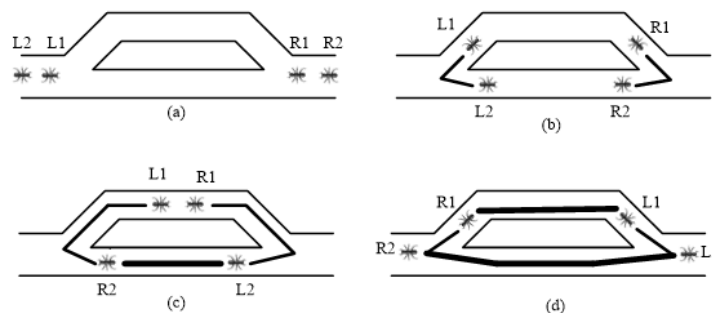


Figure 2. Stigmergy process

Figure 2 illustrates the stigmergy process. Because there is no pheromone on the existing path, the ant randomly chooses the path it will choose. Thus, some ants will choose the upper path (ants L1 and R1), and some will choose the lower path. (ants L2 and R2). When walking, each ant will put its pheromone on the path it passes, which is represented by a straight line in the path (Figure 2b) [24]. Each ant walks at a constant and the same speed. Therefore, the ants passing the lower path will arrive faster than the ants passing the upper path because the route taken is shorter (Figure 2c). From this picture, we can see that the line on the bottom lane is thicker than the top lane because the ants will go through this path faster and put down their pheromone so that the pheromone level is higher [24].

3. DIPSS OPTIMIZATION USING ACO

3.1. 9 Bus 3 Generator Multiengine System

The simulated electric power system is a 9 bus 3 generator multiengine system [25]. The image of the single-line system being tested can be seen in Figure 3.

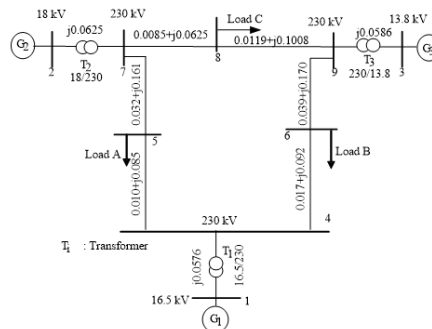


Figure 3. 9 bus 3 generator multiengine system

3.2. Using ACO in DIPSS Tuning

ACO implementation is used to tune the gain K_{s1}, K_{s2} dan K_{s3} and time constant ($T_1, T_2, T_3, T_4, T_5, T_{10}$) of DIPSS. The results of this tuning are then analyzed to get a good response. The complete ACO parameter settings used in this optimization method are shown in the Table. 1.

Table 1. ACO parameter

Number of Ant	Max Iteration	Evaporated Constant (ρ)
10	50	0.1

The condition of the system being compared is a system without DIPSS, DIPSS, and DIPSS-ACO. The observed system responses are the frequency response and the rotor angle. These responses will be analyzed about the application of DIPSS and the use of optimization methods to improve the overshoot and settling time values. The test to determine the effectiveness of the proposed method is to provide a test signal in the form of a change in the system by 5% of the generator capacity 1. The use of this optimization method is used to tune the washout parameter (T_{w1}, T_{w2}, T_{w3} , and T_{w4}), time constant ($T_1, T_2, T_3, T_4, T_5, T_6, T_7, T_8, T_9, T_{10}$), and gain parameters (K_{s1}, K_{s2} , and K_{s3}) from DIPSS. The simulation was carried out with 50 iterations. Figure 4 is a convergence graph obtained from the simulation. From the convergence image, it can be seen that the objective function reaches the best value in the 8th iteration. The best objective function shows that the ant has found the best path. The best path indicates that the DIPSS tuning is optimal. The steps of the ant colony optimization algorithm include:

Step 1 : Parameter initialization

Step 2 : Make a tour

Step 3 : Update local pheromone

Step 4 : Find the length of each tour using the formula $minimum\ error = \sum \int_0^{t_1} t|\Delta rotor\ speed(t, X)|dt$ [26]

Step 5 : Global pheromone update

Step 6 : Meets the criteria. If not, go back to step 2

Step 7 : Plot the DIPSS values

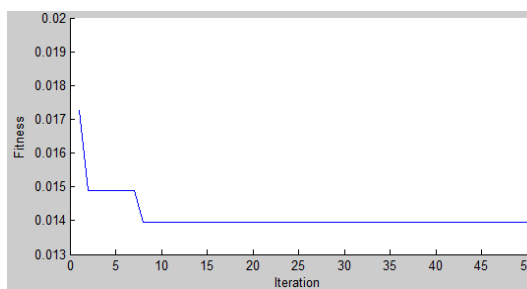


Figure 4. Convergence graph

Table 2. DIPSS parameter value results

K_{s1}	14.44	T_1	0.5169	T_8	0.328
K_{s2}	115.87	T_2	0.0101	T_9	0.714
K_{s3}	0.5807	T_3	0.7228	T_{10}	0.515
T_{w1}	102.73	T_4	0.3421		
T_{w2}	143.82	T_5	0.2301		
T_{w3}	117.89	T_6	79.09		
T_{w4}	137.58	T_7	128.4		

4. SIMULATION RESULTS

Simulation of a 9 bus 3 generator multiengine electric power system using DIPSS-ACO was observed in 20 seconds. The disturbance given to generator one is 0.05 p.u. In Figure 5, it can be seen that the change in the frequency of generator 1 for the system overshoot value without DIPSS is 0.00035 p.u, the system with DIPSS is equal to 0.0004 p.u, while the system with DIPSS tuned with ACO is 0.00032 p.u. Thus, the settling time value of generator one without DIPSS is more than 11.5 seconds, the system with DIPSS is 8.7 seconds, and the system with DIPSS tuned with ACO has the best settling time of 7.9 seconds. From these results it can be stated that DIPSS with ACO can provide additional controller signal to the excitation system.

The response of generator 2 to disturbance changes in generator 1 can be seen in Figure 6. The data obtained is the overshoot of the system without DIPSS of 0.00046 p.u, with DIPSS of 0.00048 p.u, and with DIPSS tuned with ACO, the best value is 0.00024 p.u. The value of system settling time is 11.5 seconds if the system is without DIPSS, 8.7 seconds if using DIPSS, and 4.4 seconds if using DIPSS tuned with ACO. It is evident that by using ACO the parameter of DIPSS can be optimally design. Hence, the DIPSS can transform their input and produce optimal output that can be used to modulate the excitation system of the generator. By modulatiomg the excitation system, the exciation system can produce the magnetic field that required for the system.

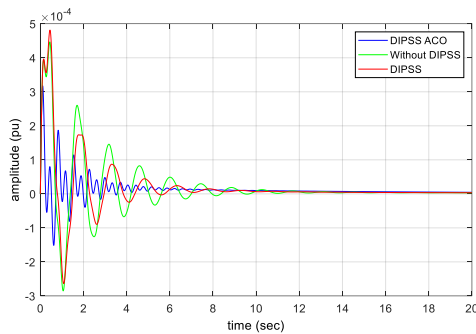


Figure 5. Generator 1 frequency change

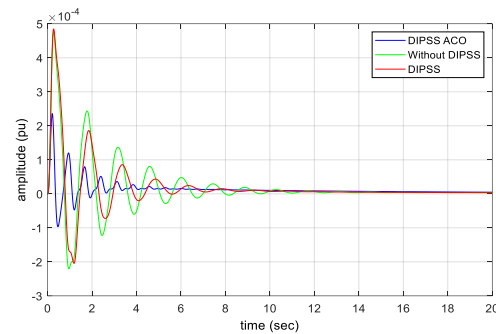


Figure 6. Generator 2 frequency change response

The frequency response of generator 3 is still affected by disturbances that occur in generator 1. This can be seen in Figure 7. The value of the system frequency overshoot can be seen from Figure 7, which is 0.00057 p.u without DIPSS, 0.00058 p.u with DIPSS, and the best is 0.00029 p.u with DIPSS-ACO. The value of settling time is more than 11.5 seconds if, without DIPSS, 8.7 seconds if using DIPSS, and the best value is 7.8 seconds if using DIPSS-ACO. Similar with frequency response of generator 1 and 2, the response of generator 3 is also shows that ACO can provide optimal value for DIPSS.

To shows the efficacy of ACO compared to the other algorithm method is done by comparing the execution time of each algorithm for designing DIPSS. Three different algorithms namely ant colony optimization, grey wolf optimizer (GWO), and particle swarm optimization (PSO) are compared in this paper. Figure 8 shows the comparison between ACO, GWO and PSO in terms of execution time. It is observed that ACO is the fastest compared to the other algorithm for finding the best parameter of DIPSS.

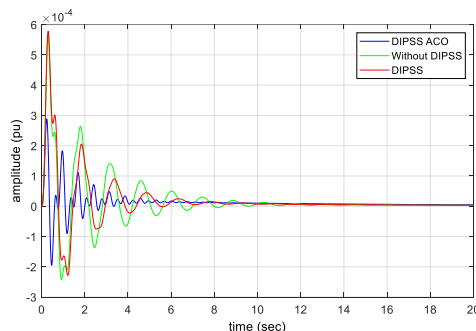


Figure 7. Generator 3 frequency change response

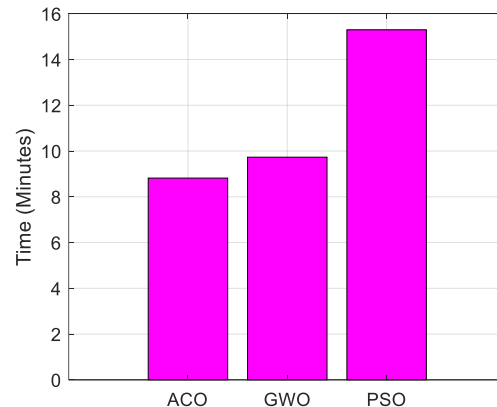


Figure 8. Execution time comparison

5. CONCLUSION

This paper proposed a method for enhancing dynamic stability of power system by modulating the excitation system of the generator using additional controller. The additional controller used in this paper is dual input power system stabilizer. To get the optimal parameter of DIPSS metaheuristic approach called ant colony optimization (ACO) is used. From the simulation results it is found that ACO can provide an optimal parameter of DIPSS for enhancing dynamic stability of power system. These are indicated by smallest overshoot for all generator compared to the other scenarios. In addition, ACO is also giving fastest execution time compared to the other method (around 8 minutes).

REFERENCES

- [1] A. U. Krismanto, N. Mithulananthan, H. Setiadi, E. Y. Setyawan, and M. Abdillah, "Impacts of grid-tied microgrid on stability and interaction of power systems considering RE uncertainties," *Sustainable Energy, Grids and Networks*, vol. 28, p. 100537, 2021.
- [2] R. K. Khadanga and J. K. Satapathy, "Time delay approach for PSS and SSSC based coordinated controller design using hybrid PSO–GSA algorithm," *International Journal of Electrical Power & Energy Systems*, vol. 71, pp. 262–273, 2015, doi: <https://doi.org/10.1016/j.ijepes.2015.03.014>.
- [3] H. Setiadi *et al.*, "An Extreme Learning Machine Based Adaptive VISMA for Stability Enhancement of Renewable Rich Power Systems," *Electronics*, vol. 11, no. 2, p. 247, 2022.
- [4] X. Y. Bian, Y. Geng, K. L. Lo, Y. Fu, and Q. B. Zhou, "Coordination of PSSs and SVC Damping Controller to Improve Probabilistic Small-Signal Stability of Power System With Wind Farm Integration," *IEEE Transactions on Power Systems*, vol. 31, no. 3, pp. 2371–2382, 2016, doi: 10.1109/TPWRS.2015.2458980.
- [5] H. Setiadi *et al.*, "Influence of Adding BESS as Ancillary Controller of Wind Power Plant on Low Frequency Oscillation," *International Journal of Intelligent Engineering and Systems*, vol. 14, no. 5, pp. 188–198, 2021.
- [6] S. Robak and K. Gryspanowicz, "Rotor angle small signal stability assessment in transmission network expansion planning," *Electric Power Systems Research*, vol. 128, pp. 144–150, 2015, doi: <https://doi.org/10.1016/j.epr.2015.07.003>.
- [7] Y. Shen, W. Yao, J. Wen, H. He, and L. Jiang, "Resilient Wide-Area Damping Control Using GrHDP to Tolerate Communication Failures," *IEEE Transactions on Smart Grid*, p. 1, 2018, doi: 10.1109/TSG.2018.2803822.
- [8] T. Surinkaew and I. Ngamroo, "Two-level coordinated controllers for robust inter-area oscillation damping considering impact of local latency," *IET Generation, Transmission & Distribution*, vol. 11, no. 18, pp. 4520–4530, 2017, doi: 10.1049/iet-gtd.2016.2068.
- [9] S. Gurung, F. Jurado, S. Naetiladdanon, and A. Sangswang, "Comparative analysis of probabilistic and deterministic approach to tune the power system stabilizers using the directional bat algorithm to improve system small-signal stability," *Electric Power Systems Research*, vol. 181, p. 106176, 2020.
- [10] J. Hartono, N. Hariyanto, F. S. Rahman, T. Kerdphol, M. Watanabe, and Y. Mitani, "Power System Stabilizer Tuning to Enhance Kalimantan Selatan - Tengah and Kalimantan Timur System Interconnection Stability Using Particle Swarm Optimization," in *2018 5th International Conference on Electric Power and Energy Conversion Systems (EPECS)*, 2018, pp. 1–6. doi: 10.1109/EPECS.2018.8443361.
- [11] D. Chitara, K. R. Niazi, A. Swarnkar, and N. Gupta, "Cuckoo Search Optimization Algorithm for Designing of a Multimachine Power System Stabilizer," *IEEE Transactions on Industry Applications*, vol. 54, no. 4, pp. 3056–3065, 2018, doi: 10.1109/TIA.2018.2811725.
- [12] "IEEE Recommended Practice for Excitation System Models for Power System Stability Studies," *IEEE Std 421.5-2016 (Revision of IEEE Std 421.5-2005)*, pp. 1–207, 2016. doi: 10.1109/IEEESTD.2016.7553421.
- [13] V. Vittal, J. D. McCalley, P. M. Anderson, and A. A. Fouad, *Power system control and stability*. John Wiley & Sons, 2019.
- [14] R. Devarapalli, B. Bhattacharyya, N. K. Sinha, and B. Dey, "Amended GWO approach based multi-machine power system stability enhancement," *ISA transactions*, vol. 109, pp. 152–174, 2021.
- [15] A. Nateghi and H. Shahsavari, "Optimal Design of $FPI^{\lambda} D^{\mu}$ based Stabilizers in Hybrid Multi-Machine Power System Using GWO Algorithm," *Journal of Operation and Automation in Power Engineering*, vol. 9, no. 1, pp. 23–33, 2021.
- [16] H. Setiadi, A. Swandaru, D. A. Asfani, T. H. Nasution, M. Abdillah, and A. U. Krismanto, "Coordinated Design of DIPSS and CES Using MDEA for Stability Enhancement: Jawa-Bali Indonesian Power Grid Study Case".
- [17] M. Singh, R. N. Patel, and D. D. Neema, "Robust tuning of excitation controller for stability enhancement using multi-objective metaheuristic Firefly algorithm," *Swarm and Evolutionary Computation*, 2018, doi: <https://doi.org/10.1016/j.swevo.2018.01.010>.
- [18] H. Setiadi, N. Mithulananthan, A. U. Krismanto, and I. Kamwa, "Optimization based Design of Dual Input PSS for Improving Small Signal Stability of Power System with RESS.," *International Journal on Electrical Engineering & Informatics*, vol. 11, no. 4, 2019.
- [19] I. Kamwa, R. Grondin, and G. Trudel, "IEEE PSS2B versus PSS4B: the limits of performance of modern power system stabilizers," *IEEE Transactions on Power Systems*, vol. 20, no. 2, pp. 903–915, 2005.
- [20] S. Paszek and A. Nocoń, "Parameter polyoptimization of PSS2A power system stabilizers operating in a multi-machine power system including the uncertainty of model parameters," *Applied Mathematics and Computation*, vol. 267, pp. 750–757, 2015, doi: <https://doi.org/10.1016/j.amc.2014.12.013>.

- [21] Y. Yao, Y. Hong, D. Wu, Y. Zhang, and Q. Guan, "Estimating the effects of 'community opening' policy on alleviating traffic congestion in large Chinese cities by integrating ant colony optimization and complex network analyses," *Computers, Environment and Urban Systems*, vol. 70, pp. 163–174, 2018, doi: <https://doi.org/10.1016/j.compenvurbsys.2018.03.005>.
- [22] J. Zhou *et al.*, "A multi-objective multi-population ant colony optimization for economic emission dispatch considering power system security," *Applied Mathematical Modelling*, vol. 45, pp. 684–704, 2017, doi: <https://doi.org/10.1016/j.apm.2017.01.001>.
- [23] M. Taufik, D. Lastomo, and H. Setiadi, "Small-disturbance angle stability enhancement using intelligent redox flow batteries," in *2017 4th International Conference on Electrical Engineering, Computer Science and Informatics (EECSI)*, 2017, pp. 1–6. doi: 10.1109/EECSI.2017.8239143.
- [24] L. Bianchi, M. Dorigo, L. M. Gambardella, and W. J. Gutjahr, "A survey on metaheuristics for stochastic combinatorial optimization," *Natural Computing*, vol. 8, no. 2, pp. 239–287, 2009, doi: 10.1007/s11047-008-9098-4.
- [25] S. Panda, "Differential evolutionary algorithm for TCSC-based controller design," *Simulation Modelling Practice and Theory*, vol. 17, no. 10, pp. 1618–1634, 2009.
- [26] H. Setiadi, N. Mithulananthan, and R. Shah, "Design of wide-area POD with resiliency using modified DEA for power systems with high penetration of renewable energy," *IET Renewable Power Generation*, vol. 13, no. 2, pp. 342–351, 2018.

APPENDIX

Symbol	Meaning	Symbol	Meaning
K_1, K_2, K_4, K_5, K_6	The functions of the operating real and reactive loading as well as the excitation levels in the generator	T_{tu}	Time constant of turbine
C_3	A function of ratio of impedance	T_w	Time constant for washout filter
K_A	Amplifier gain	T'_{do}	Time constant for generator field
K_E	Exciter gain	X_e	Equivalent reactance of transmission line
K_F	Filter gain	Z_{eq}	Equivalent impedance
K_{gw}	Gain of governor	$\Delta E'_q$	Voltage generator deviation
δ_i	Rotor angle	ΔT_e	Electrical torque deviation
M	2x Inertia constant	ΔT_G	Governor output deviation
R_e	Equivalent resistance of transmission line	ΔT_m	Mechanical torque deviation
T_A	Time constant of amplifier	ΔV_A	Voltage deviation of amplifier
T_E	Time constant of exciter	ΔV_F	Voltage deviation of filter
T_F	Time constant of filter	ΔV_{FD}	Voltage field deviation
T_{gu}	Time constant of governor	ΔV_{Le}	Voltage output of washout filter
T_r	Time constant of transducer	ΔV_R	Transducer voltage deviation
t_{sim}	The time simulation	ΔV_{REF}	Voltage reference
ΔV_t	Terminal voltage of generator		
$\Delta \omega$	Rotor speed deviation		